AAPS Open

RESEARCH Open Access

Strategies to stabilize dalbavancin in aqueous solutions: Section 4—identification of heat degradation products in 2-hydroxypropyl-β-cyclodextrin and divalent metal ion solutions at pH 4.5 and 7.0

Sardar M. Jakaria[1,2*], David E. Budil[2] and James Murtagh[1]

Abstract

Heat stress studies have been conducted in support of developing a heat-stable liquid solution of dalbavancin. The degradation products that form in heat-stressed buffered dalbavancin solutions have been identified, including the known major degradation product, mannosyl aglycone (MAG), and four previously uncharacterized compounds. Liquid chromatography-mass spectrometry/mass spectrometry (LC–MS/MS) was used to identify the degradation products of dalbavancin in acetate- and phosphate-buffered solutions under thermal stress at 70 °C and the changes in the degradation pattern in the presence of 2HPβCD and divalent metal ions. Although Ca^{2+}, Mg^{2+}, and Zn^{2+} did not reduce dalbavancin degradation under thermal stress in acetate buffer, 2HPβCD significantly reduced its overall degradation, in particular, the formation of MAG. This protective effect was enhanced by the addition of Ca^{2+} to the formulation. In phosphate buffer, MAG formation was also reduced by the addition of 2HPβCD, although significant increases in other degradation products were observed in this case. The addition of Mg^{2+} to 2HPβCD significantly reduced the overall degradation while increasing MAG formation somewhat. The results strongly suggest that 2HPβCD forms a complex with the hydrophobic glycone tail of dalbavancin, suppressing hydrolysis of the glycosidic bond.

Introduction

Dalbavancin (a second-generation lipoglycopeptide antibiotic) is the only approved FDA product for treating infections caused by susceptible strains of *Streptococcus aureus* including MRSA, *Streptococcus pyogenes*, *Streptococcus agalactiae*, and the *Streptococcus anginosus* group (Leuthner et al. 2016). In addition, dalbavancin is an emerging treatment option for most of the MRD/XRD microorganisms which are Gram-positive cocci bacteria (Giurazza et al. 2021). Dalbavancin is derived from a natural product glycopeptide by amidation of the peptide-carboxy group of amino acid 7 with 3-(dimethylamino)-1-propylamine (Blaskovich et al. 2018). Like other lipoglycopeptides, dalbavancin targets the *C*-terminal *acyl*-d-Ala-d-Ala subunit of peptidoglycan precursors in the cell wall of Gram-positive bacteria. The origin, structure, in vitro and in vivo characterization, and biosynthesis of dalbavancin have been reported (Malabarba and Ciabatti 2001; Ziora et al. 2014; Cheng et al. 2014; DALVANCE 2014; Scheinfeld 2006; Stogniew et al. 2012); however, the structures of the degradation

*Correspondence:
Sardar M. Jakaria
sjakaria@hikma.com
[1] Hikma Pharmaceuticals, Bedford, OH 44146, USA
[2] Department of Chemistry and Chemical Biology, Northeastern University, Boston, MA 02115, USA

products of this important drug have not been reported. Dalbavancin (Fig. 1) is a mixture of five closely related active homologs or factors (A0, A1, B0, B1, and B2). The B0 factor is the major component of dalbavancin (DALVANCE 2014).

Dalbavancin is unstable in aqueous solutions (Stogniew et al. 2012) which has motivated studies to develop a heat-stable solution formulation of dalbavancin. Standards for studies to test the heat stability of drugs for distribution in climate zones III (hot/dry) and IV (hot/humid or tropical) have been proposed by the International Conference on Harmonization or ICH (Grimm 1998). Specifically, 40 °C for 6 months was selected to cover the extreme temperatures that can occur in these climatic zones. In the present work, a standard degradation study was carried out at 40 °C and repeated at 70 °C. The goal of the higher temperature study was to speed up the formation of degradation and boost their yields sufficiently to enable the identification of as many as possible by LC–MS/MS. The degradants identified at 70 °C include those observed at the standard testing temperature in addition to several that have not been previously observed. The results provide new details about the stabilizing effect of divalent metal ions and 2-hydroxypropyl-β-cyclodextrin (2HPβCD) on dalbavancin in acetate and phosphate buffers.

Materials and methods

Materials

All materials used in this study were commercially available chemicals or reagents. Dalbavancin hydrochloride reference standards, including standards for its A0, B0, and B1 isoforms as well as MAG (DB-R1) and DB-R2 impurity standards, were obtained from a company with a Drug Master File. Other chemicals or reagents included 2-hydroxproyl-β-cyclodextrin (2HPβCD), monobasic sodium phosphate, phosphoric acid, calcium chloride, magnesium chloride, zinc chloride, reagent-plus or ACS grade sodium hydroxide, ammonium acetate, acetic acid, hydrochloric acid, HPLC-grade acetonitrile, and type 1 ultra-pure water from a commercially available water purification system.

Formulation and thermal stress studies

Dalbavancin formulations were prepared for stability testing by combining a concentrated buffer solution with stock solutions of dalbavancin and 2HPβCD, $MgCl_2$, $CaCl_2$, or $ZnCl_2$ in water, in the amounts needed to produce the desired compositions and final concentrations after diluting with water in a volumetric flask, which are summarized in Table 1. The final dalbavancin concentration was 20 mg/mL in all samples. The pH of the acetate and phosphate buffer formulations was adjusted to 4.5 and 7.0, respectively.

The following codes designate the formulations used: The first characters refer to the type of buffer: AcB (acetate) and Phosp (phosphate). The following digits refer to the buffer concentration in mM, the type of metal ion followed by its concentration in mM, and 2HPβCD followed by its concentration in mM. For example, AcB-10Ca10Cyclod55 designates 10 mM acetate buffer (pH 4.5), 10 mM $CaCl_2$, and 55 mM 2HPβCD. The prepared

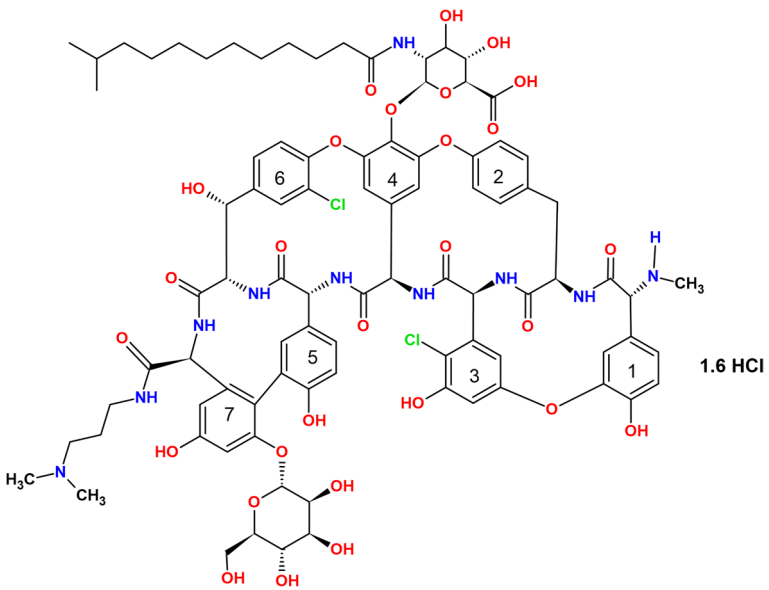

Fig. 1 Dalbavancin structural formula (DALVANCE 2014)

Table 1 Composition of 20 mg/mL (11 mM) dalbavancin liquid formulations in 10 mM acetate buffer (pH 4.5) and 10 mM phosphate buffer (pH 7.0)

Dalbavancin solution ID	Metal ion	2HPβCD
AcB10	None	None
AcB10Ca10	Ca^{2+} 10 mM	None
AcB10Mg2	Mg^{2+} 2 mM	None
AcB10Zn2	Zn^{2+} 2 mM	None
AcB10Cyclod55	None	55 mM
AcB10Ca10Cyclod55	Ca^{2+} 10 mM	55 mM
Phosp10[a]	None	None
Phosp10Cyclod110	None	110 mM
Phosp10Mg50Cyclod110	Mg^{2+} 50 mM	110 mM

[a] Dalbavancin precipitated in phosphate buffer solution without 2HPβCD

solutions were stored in 6R glass type 1 vials for 5 days (acetate samples) and 3 days (phosphate samples) at 70 °C and protected from light.

The stability of the formulations listed in Table 1 was first assessed following the ICH guidelines for long-term and accelerated stability studies for climatic zones III and IV (Grimm 1998). The samples were stored in 6R glass type 1 vials for 6 months at 40 °C and protected from light, after which the degradation products were assessed by the RP-HPLC method described in the "Reversed-phase high-performance liquid chromatography (RP-HPLC) method" section. However, this standard 6-month stability study did not produce degradants in sufficient quantity for satisfactory secondary analysis by the HPLC–MS/MS method described in the "Reversed-phase high-performance liquid chromatography-mass spectrometry (HPLC–MS/MS) method" section. Therefore, degradation studies were repeated at a much higher temperature of 70 °C in order to produce the degradants rapidly and in sufficient quantities for MS/MS analysis.

All solutions for the higher temperature study were stored at 5 °C for 4 weeks. Formulations in acetate buffer were stressed at 70 °C for 5 days. Based on a preliminary finding that dalbavancin is less heat stable in phosphate buffer than in acetate, samples in phosphate buffer were stressed at the same temperature for only 3 days. The samples were diluted to 1 mg/mL with method diluent prior to analysis. The initial dalbavancin concentration was determined by using the HPLC–UV method at 280 nm for both the 40 °C and the 70 °C studies.

Reversed-phase high-performance liquid chromatography (RP-HPLC) method

Dalbavancin recovery (remaining dalbavancin as a percentage of the initial amount) was determined by the RP-HPLC method. Chromatographic separation of dalbavancin and its degradation products was performed on a commercially available HPLC system equipped with a pump, photodiode array detector, autosampler, and column oven. For analytical HPLC, a commercially available, C18 column (250 × 4.6 mm, 5 µm particle size, USP L-1 column packing) was used for the separation of all known and unknown impurities from dalbavancin. The in-house stability-indicating method that was used to separate the degradation products of dalbavancin utilized mobile phases A and B. Mobile phase A was a 90:10 (v/v) ratio of buffered solution and acetonitrile where the buffered solution consisted of 6.0 g of anhydrous sodium dihydrogen phosphate in 1 L ultra-pure water at pH 6.0 adjusted with sodium hydroxide. The mobile phase B was a 30:70 ratio of the buffered solution described above and acetonitrile. The initial composition of mobile phases A and B was 80:20 (v/v). The amount of mobile phase B was then increased to 33% over a 7-min period and was maintained at this level for 33 min and then increased to 45% over a 15-min period and again increased to 90% over a 5-min period and maintained at this level for 7 min prior to returning to the initial mobile phase composition over a 1-min period and equilibrated for a 12-min period (Table 2). Before the first sample injection, the column was allowed to equilibrate for approximately 60 min. For both assay and impurity methods, samples were kept at 5 °C in an autosampler, and the chromatography was performed at a column temperature of 50 °C, a flow rate of 1.0 mL/min, and a sample injection volume of 10 µL. The chromatograms were obtained at 280 nm for the assay and 220 nm for the impurity method. The sample concentration was ~ 1.0 mg mL^{-1} prepared in the diluent in a 70:30 ratio of water and acetonitrile for the degradation study.

Table 2 HPLC method gradient program

Time (min)	% mobile phase A	% mobile phase B
0	80	20
7	67	33
40	67	33
55	55	45
60	10	90
67	10	90
68	80	20
80	80	20

Reversed-phase high-performance liquid chromatography-mass spectrometry (HPLC–MS/MS) method

The samples at 1 mg/mL in method diluent were subjected to LC–MS/MS analysis to identify the degradation

products. LC–MS/MS analysis was performed on a commercially available linear ion trap mass spectrometer coupled with an HPLC system consisting of a low-pressure quaternary degasser, autosampler, and column oven. The HPLC was conducted as described in the "Reversed-phase high-performance liquid chromatography (RP-HPLC) method" section, and LC–MS compatible mobile phases A and B were used. Mobile phase A was a 90:10 (v/v) ratio of buffered solution and acetonitrile where the buffered solution consisted of 0.77 g of ammonium acetate in 1 L ultra-pure water at pH 5.5 adjusted with acetic acid. The mobile phase B was a 30:70 ratio of the buffered solution described above and acetonitrile. The gradient was the same as described in the "Reversed-phase high-performance liquid chromatography (RP-HPLC) method" section and Table 2, where the initial composition of mobile phases A and B was 80:20 (v/v). The amount of mobile phase B was then increased to 33% over a 7-min period and was maintained at this level for 33 min and then increased to 45% over a 15-min period and again increased to 90% over a 5-min period and maintained at this level for 7 min prior to returning to the initial mobile phase composition over a 1-min period and equilibrated for a 12-min period. Before the first sample injection, the column was allowed to equilibrate for approximately 60 min. A commercially available C18 column (250 × 4.6 mm, 5 µm particle size, USP L-1 column packing) was used for the separation of all known and unknown impurities from dalbavancin. The analysis was done in a positive electrospray ionization (ESI) mode under the following conditions: ion source voltage (IS) = 8 kV, source heater temp = 75 °C, capillary temperature = 350 °C, and sheath gas flow = 15 units, where nitrogen was used as sheath gas and helium as collision gas. Mass fragmentation studies were carried out by maintaining normalized collision energy at 35 V with an *m/z* range of 500–1900 amu.

Results

Degradation products of dalbavancin in acetate (pH 4.5) and phosphate (pH 7.0) buffers

The presentation in this section will focus first on the identification of degradation products from accelerated studies at 70 °C and how the product yields are modulated by commonly used excipients such as Mg^{2+}, Ca^{2+}, Zn^{2+}, and 2HPβCD. The section will conclude with a comparison of these findings with the products observed at 40 °C.

LC/MS analysis was first carried out on dalbavancin in only acetate (pH 4.5) and phosphate (pH 7.0) buffers without excipients, as shown in Figs. 2 and 3, respectively. The liquid chromatogram traces in the two buffers (Figs. 2a and 3a) are quite similar, exhibiting eight major peaks. The total ion chromatograms for both solvents that are shown respectively in Figs. 2b, c and 3b confirmed that the eight peaks in the LC trace arise from ions in the *m/z* range of 1400–1850 Da. These spectra were compared to a formulation of dalbavancin with only 2HPbCD. Interestingly, in this formulation, one of the peaks (peak 4 at a retention time of 25.34 min) was inhibited, while an additional peak appeared at a retention time of 29.23 min, labeled 4a in Fig. 3c.

Three of the nine peaks observed by LC-UV, peaks 4, 5, and 6 in Figs. 2a and 3a, could be identified with known homologs of dalbavancin (Zhu et al. 2020) by their masses and retention times and were therefore not degradation products. Respectively, these peaks corresponded to isoforms A1, B0 (the primary form of dalbavancin), and B1, all with *m/z* = 1817.7 Da for the singly protonated ion, as confirmed by comparison with reference standard compounds. A representative mass spectrum of peak 5, the B0 isoform, is shown in Fig. 4a.

Two more of the nine peaks could be identified with known impurities in dalbavancin preparations, both by their molar mass and by comparison with available impurity standards. Compound 1 with an *m/z* $[M+H]^+$ of 1460.6 Da (Fig. 4b) was identified as mannosyl aglycone (MAG), the major degradation product of dalbavancin (Stogniew et al. 2012). A comparison of the LC/MS spectrum of compound 1 with the MAG standard is given in the supplemental material (SM) as Fig. SM 1.

Compound 4a, which only appeared when dalbavancin was heat stressed in the presence of 2HPβCD, has the same *m/z* $[M+H]^+$ as dalbavancin. Figure 4c shows the extracted ion chromatogram for this *m*/z value, which exhibited peaks corresponding to compounds 4a and dalbavancin. Comparison with an impurity standard (Fig. SM 2) identified compound 4a as the previously characterized impurity DB-R2 from a commercial source with a Drug Master File. This compound is a diastereomer of dalbavancin, differing only by the epimerization of the alpha carbon of residue 3 of the peptide.

The remaining four peaks in the LC-UV trace corresponded to degradation products that had not previously been reported. Peaks 2 and 3 had the same *m/z* $[M+H]^+$ value of 1447.3 Da, and peaks 7 and 8 had the same *m/z* $[M+H]^+$ value of 1804.5 Da. These assignments were confirmed by the extracted ion chromatograms constructed from these two *m/z* values as shown in Fig. 5, which reproduced the peaks observed in the LC. The UV, MS, and MS/MS spectra from peaks 2, 3, 7, and 8 appear respectively in Fig. SM 3, Fig. SM 4, Fig. SM 5, and Fig. SM 6. The UV spectra and patterns of secondary and tertiary fragments for compounds 2 and 3 were very similar (compare Fig. SM 3 and Fig. SM 4), suggesting that they are diastereomers. These compounds were designated as DB-DP1 stereoisomers. Similarly, comparisons of the

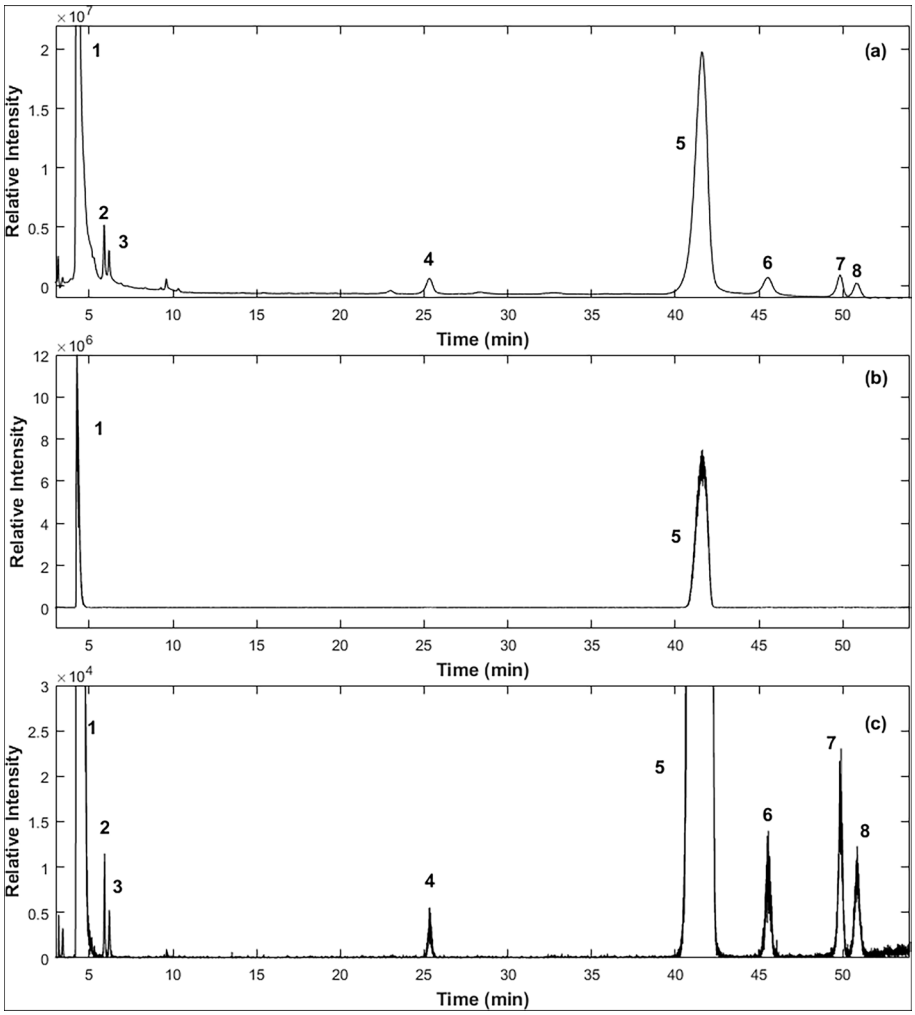

Fig. 2 **a** LC – UV trace, **b** total ion chromatogram (*m/z* 1400–1850) of heat-stressed dalbavancin (full scale), and **c** total ion chromatogram (*m/z* 1400–1850) of stressed dalbavancin (400 × expanded view) in acetate buffered solution (AcB10)

UV spectra and patterns of secondary, tertiary, and quaternary fragments for compounds 7 and 8 (compare Fig. SM 5 and Fig. SM 6) suggest that these compounds were also diastereomers, and they were designated as DB-DP2 stereoisomers. The assignment of compounds 2, 3, 7, and 8 to specific stereoisomers of DB-DP1 and DB-DP2 is made in the "Assignment of DB-DP1, DB-Iso-DP1, DB-DP2, and DP-Iso-DP2" section. The retention times and mass-to-charge ratio (*m/z*) values for all nine compounds were identified by LC–MS (Table 3).

Secondary fragments of dalbavancin

Dalbavancin degradation product structures were determined based on the *m/z* value of each component from the LC–MS data, and then, MS/MS data were used to confirm the determination as outlined in this section. MS/MS was carried out on dalbavancin as well as on the degradation products MAG, DB-DP1, DB-Iso-DP1, DB-DP2, and DB-Iso-DP2. The dalbavancin structure and its fragmentation pathways are shown in Fig. 6.

Fig. SM 7 presents the UV, MS, and MS/MS spectra of unmodified dalbavancin at *m/z* $[M+H]^+$ = 1817.65 Da and *m/z* $[M+2H]^{2+}$ = 909.51 Da. Singly ionized secondary fragments appeared at *m/z* values of 1786.54, 1655.56, 1624.51, 1460.31, 1429.34, 1267.49, and 1222.12 Da, as shown in Fig. SM 7 (c). The absence of any shifted peaks with *m/z* corresponding to dalbavancin complexed with acetate or phosphate indicates that such species were not formed in the buffers used.

Assignment of DB-DP1, DB-Iso-DP1, DB-DP2, and DP-Iso-DP2

The MS spectra of DB-DP2 and DB-Iso-DP2 (Fig. SM 5 (b) and Fig. SM 6 (b)) both exhibited major peaks at *m/z* $[M+H]^+$ = 1804.49 and *m/z* $[M+2H]^{2+}$ = 902.05 Da,

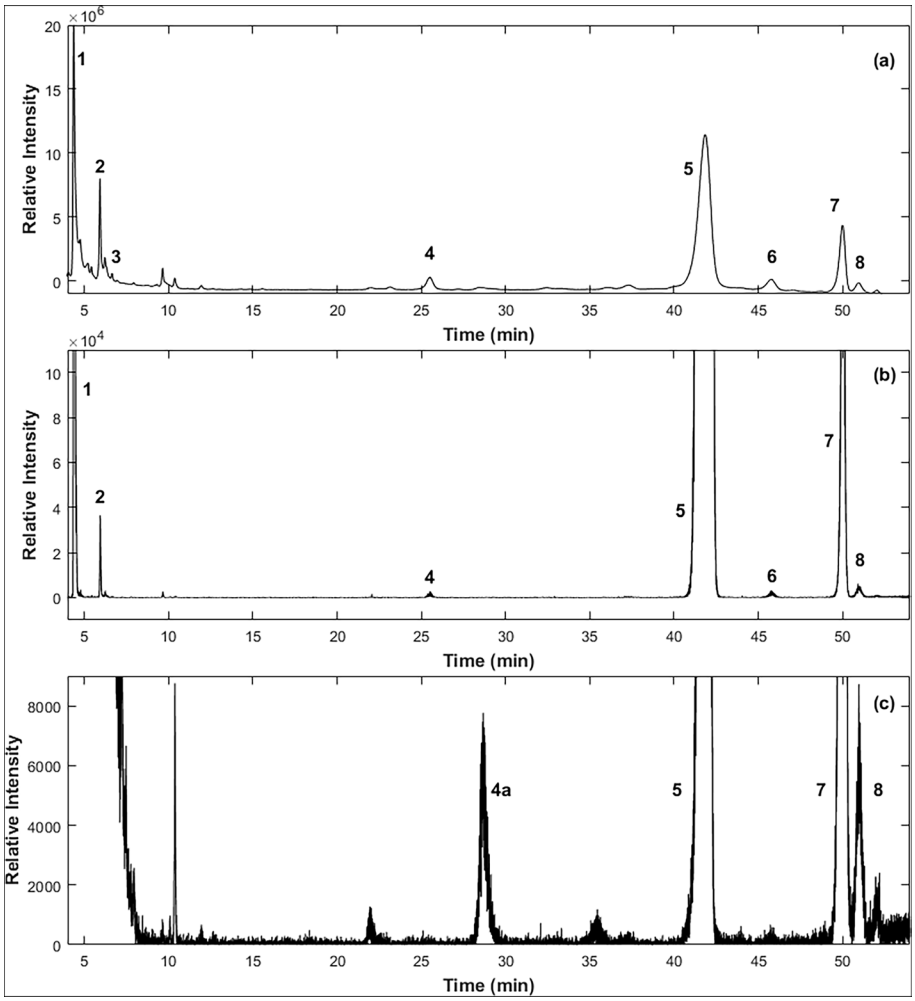

Fig. 3 **a** LC – UV trace and **b** total ion chromatogram (*m/z* 1400–1850 Da) of heat-stressed dalbavancin in phosphate buffer (Phosp10). **c** total ion chromatogram (*m/z* 1400–1850 Da) of heat-stressed dalbavancin with 2HPβCD only in phosphate buffered solution (Phosp10Cyclod110)

indicating that the molar mass of these diastereomers was approximately 13 Da less than that of dalbavancin. This most likely results from the replacement of fragment 11 (F11) in Fig. SM 5 (a) by a hydroxyl group. The MS2 (secondary fragment) spectra of both DB-DP2 diastereomers exhibited a major peak at $m/z = 1447$ Da, which was the *m/z* for DB-DP1 and its diastereomer. The identities of these primary fragment ions were confirmed by comparing their MS3 spectra (Fig. SM 3 (d) and Fig. SM 4 (d)) with the MS2 spectra of the DB-DP1 ion and its diastereomer (Fig. SM 7 (c) and Fig. SM 8 (c)). Specifically, DB-DP2 and its isomer at *m/z* 1804.5 Da produced MS/MS fragments at *m/z* 1447.5, 1430.4 ($[M+2H]^+$), 1285.4, 1267.5, 1240.3, and 1222.7 Da, while DB-DP1 and its isomer produced fragments at $m/z = 1429.5$, 1285.4, 1267.4, 1240.3, and 1222.3 Da. The identical fragmentation patterns indicate that DB-DP1 and its diastereomer must be contained within the structure of DB-DP2 and its diastereomer. This result further suggested that the site of isomerization is the same in the two pairs of compounds. The most likely site of this isomerization is the site that relates dalbavancin to the impurity DB-R2, namely epimerization of the alpha carbon of residue 3.

The peaks at *m/z* 1429.34, 1267.49, and 1222.12 Da in the MS/MS of DB-DP1 and DB-DP2 and their isomers were also characteristic fragments of dalbavancin (Fig. SM 7 (c)). The nearly identical mass spectra of dalbavancin, DB-DP1, DB-DP2, and their isomers (parts (a) of Fig. SM 9 through Fig. SM 10) suggest that the cyclic peptide core of dalbavancin is intact in all these compounds. In Fig. 7, analogous fragmentation pathways are proposed for DB-DP2 and its isomer DB-Iso-DP2.

According to the established structure of dalbavancin shown in Fig. 6a, the C_α of residue 3 is in the

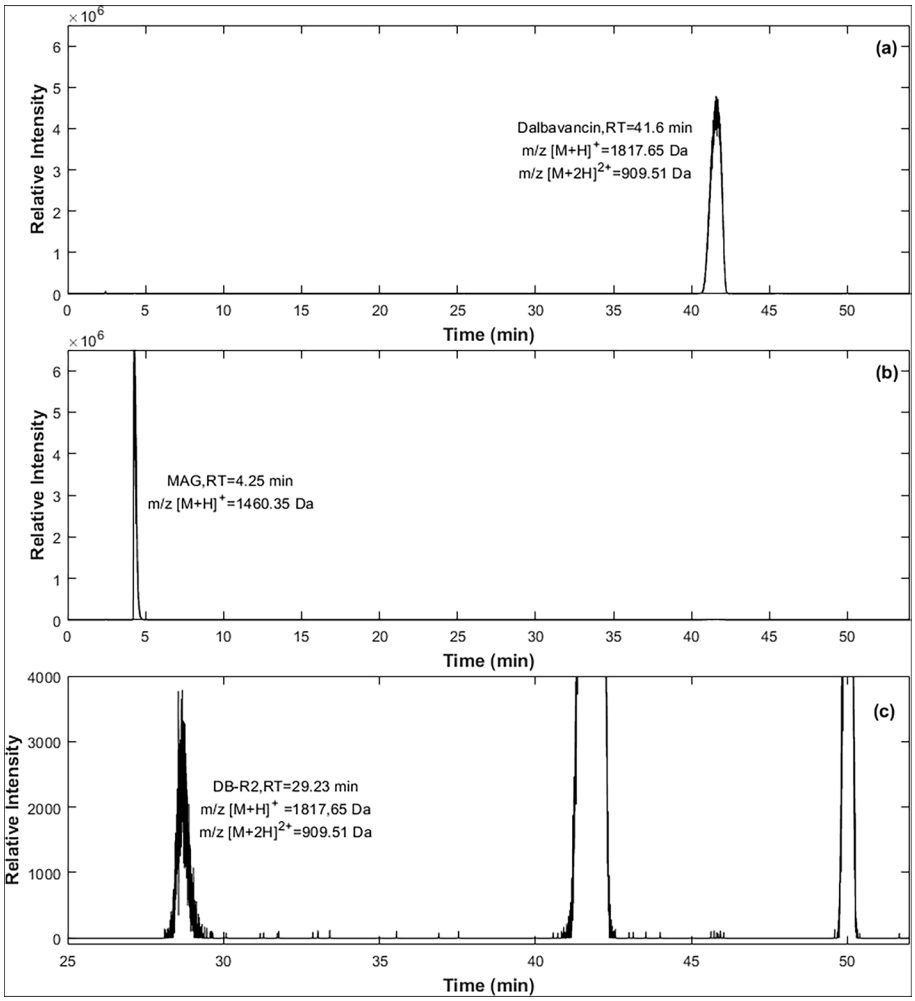

Fig. 4 Extracted ion chromatograms of **a** the ion at m/z $[M+H]^+ = 1817.65$ Da from heat-stressed dalbavancin in acetate buffer, reproducing the LC peak corresponding to compound 5 (dalbavancin). **b** The ion at *m/z* $[M+H]^+ = 1460.35$ Da from acetate buffer, reproducing the LC peak corresponding to compound 1 (MAG). **c** The ions at *m/z* $[M+H].^+ = 1817.65$ Da from heat-stressed dalbavancin in phosphate buffer with 2HPβCD, reproducing the LC peaks corresponding to compounds 4a (DB-R2) and 5 (dalbavancin)

S configuration whereas it is in the R configuration in the DB-R2 degradation product. As shown in Fig. 2 and Table 3, DB-R2 (R epimer) eluted earlier than dalbavancin (S epimer). This provided a possible basis for assigning the epimers of DB-DP1 and DB-DP2 to specific peaks in the HPLC trace. Since both compounds contained the same cyclopeptide core as dalbavancin, a change in the residue 3 C_α configuration would lead to analogous conformational changes in the peptide ring, exposing similar regions of the molecule to solvent and stationary phase. Thus, the HPLC peak of each epimer pair with the longer retention time, i.e., peaks 3 and 8, could be assigned to the S epimer analogs of dalbavancin. These compounds were designated DB-DP1 and DB-DP2. Their R epimers therefore corresponded to compounds 2 and 7 and were analogs of the impurity DB-R2; they were designated as DB-Iso-DP1 and DB-Iso-DP2, respectively.

The proposed structures for the MAG, DB-R2, DB-DP1, DB-Iso-DP1, DB-DP2, and DB-Iso-DP1 heat degradation products are depicted in Fig. 8.

Effect of divalent metal ions on dalbavancin degradation profile in acetate buffer

Figure 9 compares the recovery of dalbavancin from a selection of formulations after 5 days (for 10 mM acetate buffer at pH 4.5) or 3 days (for 10 mM phosphate buffer at pH 7.0) of incubation at 70 °C. The lowest recovery of 40% was observed in acetate buffer free of divalent metal ions and 2HPβCD (AcB10). The overall decomposition

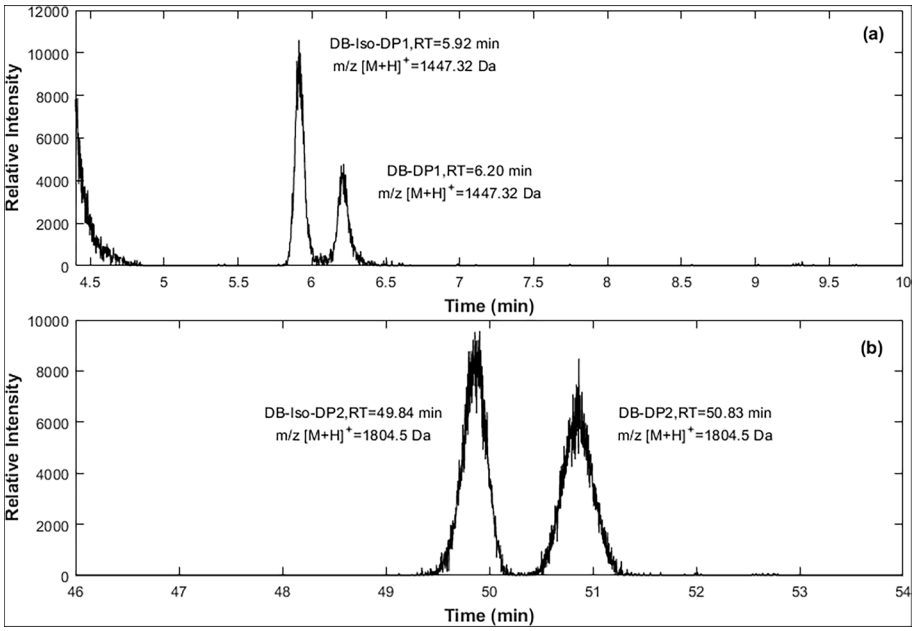

Fig. 5 **a** Extracted ion chromatograms obtained from heat-stressed dalbavancin in acetate buffer of **a** the two ions at m/z $[M+H]^+ = 1447.32$ Da reproducing the LC peaks corresponding to compounds 2 and 3, DB-Iso-DP1 and DB-DP1, respectively, and **b** the two ions at m/z $[M+H]^+ = 1804.5$ Da, reproducing the LC peaks corresponding to compounds 7 and 8, DB-Iso-DP2 and DB-DP2, respectively

Table 3 Summary of the observed degradation products of dalbavancin after stressing at 70 °C for 5 days in 10 mM acetate and 3 days in 10 mM phosphate buffer

Compound no	RT (min)	*m/z* $[M+H]^+$	Charge	Compound ID
1	4.25	1460.6	1+	Mannosyl aglycone (MAG)[a]
2	5.92	1447.32	1+	DB-Iso-DP1
3	6.20	1447.32	1+	DB-DP1
4	25.34	1817.7	1+	Dalbavancin (A1)[a,b]
4a	29.23	1817.7, 909.42	1+, 2+	DB-R2[a,c]
5	41.60	1817.7, 909.51	1+, 2+	Dalbavancin (B0)[a,b]
6	45.52	1817.7	1+	Dalbavancin (B1)[a,b]
7	49.84	1804.5	1+	DB-Iso-DP2
8	50.83	1804.5	1+	DB-DP2

[a] Identified by comparison with a standard

[b] Not a degradation product: homolog of dalbavancin

[c] Only formed in the presence of 2HPβCD with or without Mg^{2+} in phosphate buffer at pH 7

was not significantly affected by the addition of Ca^{2+}, Mg^{2+}, or Zn^{2+}: dalbavancin recovery remained near 38–40%, regardless of the identity of the divalent metal ion.

The individual heat degradation products were quantified for formulations with Ca^{2+}, Mg^{2+}, or Zn^{2+} ions using (i) the relative areas of their extracted ion chromatograph (EIC) peaks as compared to those from the acetate buffer without metal ions and (ii) the fractional area of their HPLC–UV peaks; these values are given in Table 4. Both the EIC and HPLC data showed that none of the ions significantly reduced the relative amount of MAG formation. However, both Ca^{2+} and Zn^{2+} appreciably reduced the relative amounts of DB-DP1 and DB-DP2 and their isomers, by 15–40% in the presence of Zn^{2+} and by 4–27% with Ca^{2+}. In contrast, with Mg^{2+} the reduction was only 1–4%. Since each of these four impurities constituted less than 2% of the total degradation products, the reductions shown in Table 4 did not significantly reduce the overall degradation of dalbavancin. The HPLC trace also revealed small amounts of unknown degradants that were not detected within the *m*/z range of the MS spectrum and therefore were not identified.

Effect of 2HPβCD and Ca^{2+} on dalbavancin degradation profile in acetate buffer

Figure 9 also compares dalbavancin recovery after 5 days at 70 °C for formulations containing 2HPβCD with or without Ca^{2+} ion in acetate buffer. In the presence of 2HPβCD, dalbavancin recovery increased dramatically to 77%; this effect was further increased to 86% recovery by the addition of Ca^{2+}. The degradant profiles of these two samples are given in Table 5, which again quantifies the amount of each degradation product using both the relative area of its extracted ion

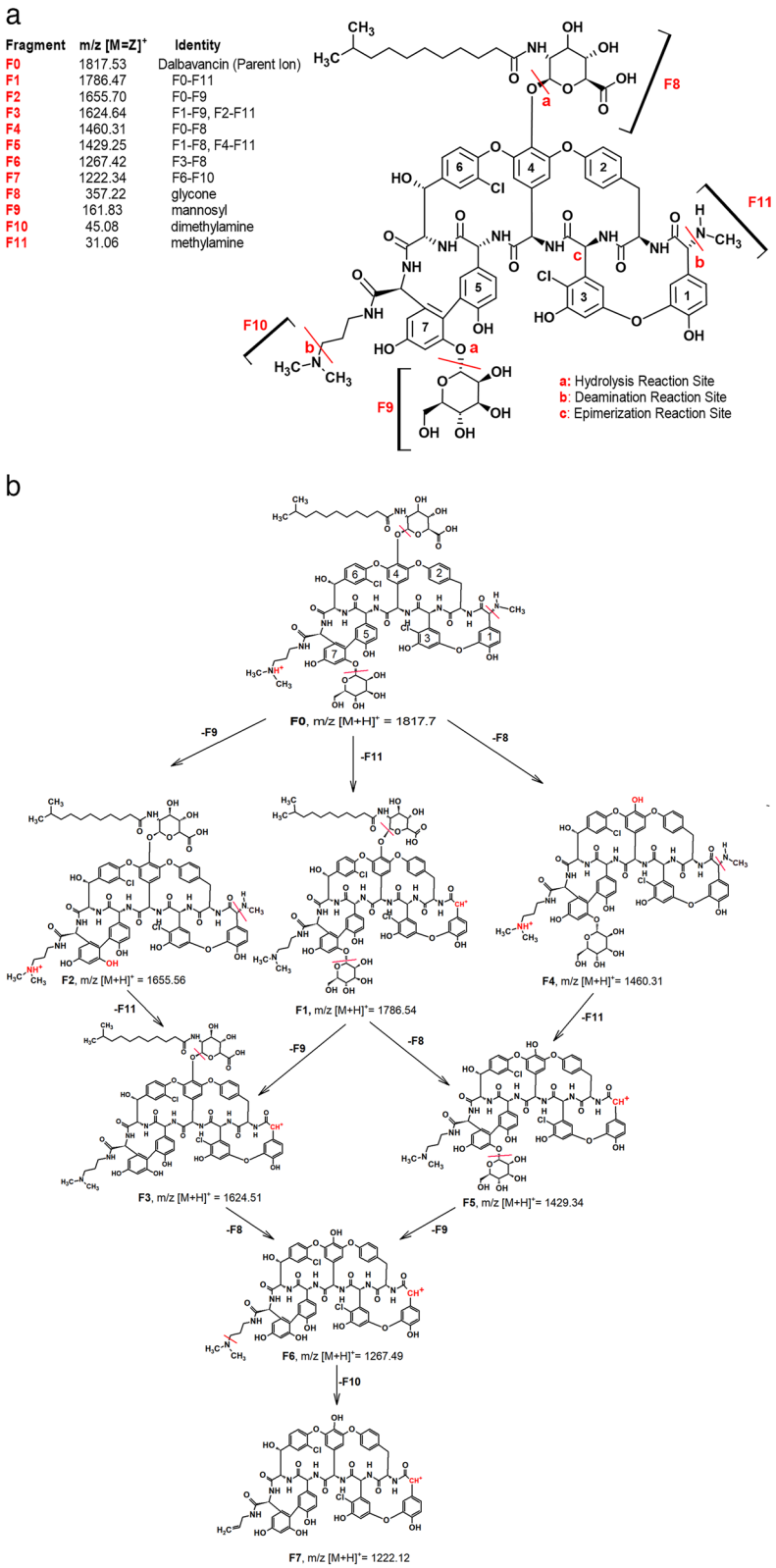

Fig. 6 **a** Cleavage/reaction sites on dalbavancin and secondary fragments observed by MS/MS; numbering of the aromatic rings as assigned in Zhu et al. (2020). **b** Structures and fragmentation pattern of secondary fragments

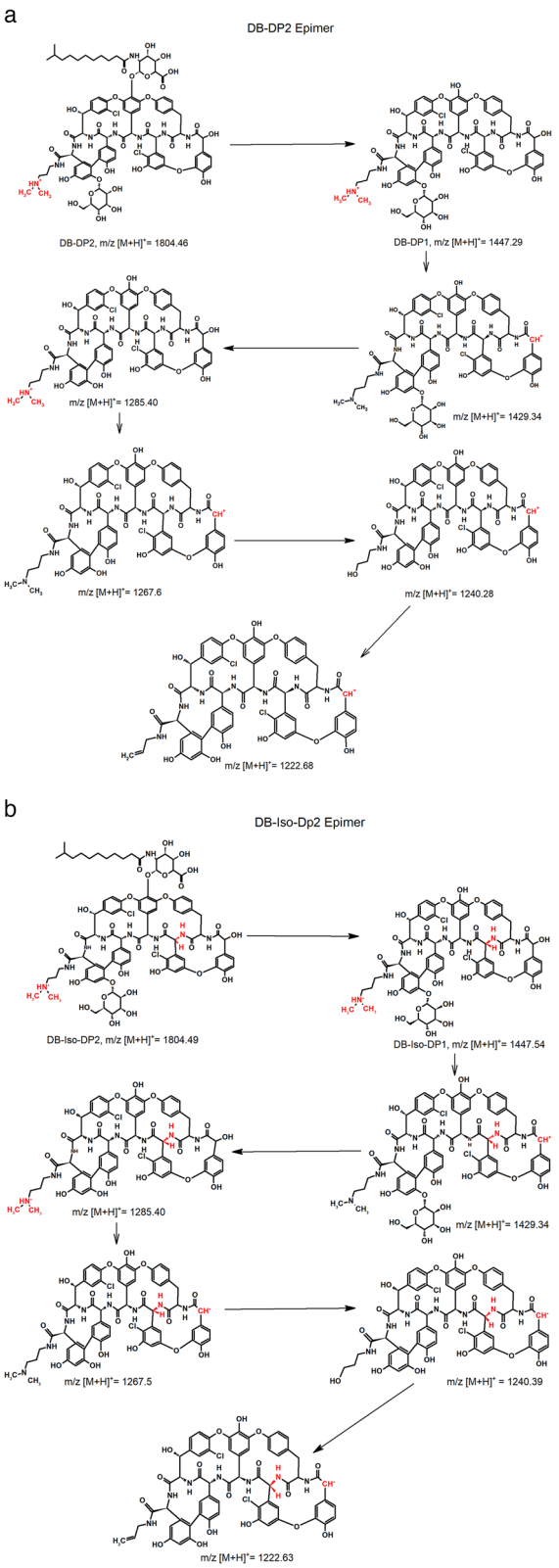

Fig. 7 Proposed fragmentation pathways of **a** DB-DP2 and its diastereomer **b** DB-Iso-DP2 showing the analogous pathways for the two epimers

chromatogram (EIC) and the relative area of its HPLC peak. 2HPβCD, either with or without Ca^{2+}, reduced the yield of all degradation products except for DB-Iso-DP1 and DB-Iso-DP2; in particular, MAG formation was reduced by 20–30%. The relative amounts of DB-Iso-DP1 and DB-Iso-DP2 were increased by 40–80%, in contrast to their stereoisomers, which were reduced by 40–70%. Since MAG was the principal degradation product, the other four impurities made only minor contributions to the overall dalbavancin degradation. Minor amounts of unidentified degradants were detected in the HPLC traces of samples with 2HPβCD in acetate, as was the case for the divalent ion studies. However, those unidentified degradants were not detected within the *m*/z range of the MS spectrum and therefore were not identified.

Effect of 2HPβCD and Mg^{2+} ion on dalbavancin degradation profile in phosphate buffer

The rightmost three bars in Fig. 9 compare dalbavancin recovery from different heat-stressed formulations in 10 mM phosphate buffer (pH 7.0). This study was motivated by our previous observation that 2HPβCD with Mg^{2+} significantly improved the stability of dalbavancin in aqueous solutions near physiological pH. As Fig. 9 shows, 56% of the dalbavancin was recovered after incubation in phosphate buffer at 70 °C for 3 days. In the presence of 2HPβCD in the same buffer, the recovery was only 27%. However, recovery was significantly increased to 70% when 2HPβCD was combined with Mg^{2+} ion, consistent with our previous results.

The degradation profile of dalbavancin in heat-stressed phosphate buffer formulations is shown in Table 6, again listing both the relative EIC peak intensity of each degradant relative to buffer alone and the fractional area under the corresponding HPLC peak for each of the samples tested. In phosphate buffer plus 2HPβCD, the amount of MAG formation was reduced relative to buffer alone, but the relative amounts of all other degradation products, particularly DB-R2, were sharply increased. Also notable was the rather large amount of unidentified degradation products produced in this formulation, which exceeded the amount of any single degradant. The addition of Mg^{2+} to this formulation reduced the formation of unidentified products but increased MAG, DB-R2, and DB-Iso-DP2 formation over that in phosphate buffer alone. The presence of Mg^{2+} did not significantly reduce the formation of other degradants except for the DB-R2, DB-Iso-DP2, and unidentified degradants relative to 2HPβCD alone. Only the HPLC–UV chromatography detected unidentified degradants, which were not present within the MS spectrum m/z range and therefore were not identified.

Comparison of results at 70 °C and 40 °C

The relative yields of degradation products observed at 70 °C and 40 °C for each of the formulations studied are presented in Table 7, expressed as peak area percentages of the total peak area under the chromatogram. Data for the 70 °C studies is reproduced from Tables 4, 5, and 6 to facilitate comparison. Reliable extracted ion chromatograms were not available from the HPLC traces obtained at 40 °C.

Identification and correspondence of the compounds appearing in the HPLC/MS chromatograms at the two temperatures were established by matching the relative retention times and molar masses of the observed peaks. Thus, MAG (DB-R1), DB-R2, and DB-Iso-DP2 were seen at both temperatures in at least some formulations whereas DB-Iso-DP1, DB-DP1, and DB-DP2 are only observed at the higher temperature. In contrast, the product DB-R6 appeared in some formulations at 40 °C but not in any formulations at 70 °C.

Discussion

High-pressure liquid chromatography with UV/visible and tandem mass spectrometric detection are the physicochemical methods most used to monitor and quantify dalbavancin in human plasma (Zhu et al. 2020; Huber et al. 2022; Alebic-Kolbah et al. 2011; Avataneo et al. 2021). The coupling of HPLC and tandem MS via an electrospray ionization (ESI) interface also allows the degradation products of drugs to be identified and quantified by extracting corresponding mass spectra from the recorded current of specific ions (Poole et al. 2011). Although the degradation products of the closely related glycopeptide vancomycin had been determined by HPLC–MS (Belissa et al. 2014; Cao et al. 2018), there had been no reported HPLC–MS studies of the stability and degradation products of dalbavancin in the pharmaceutical dosage form. This motivated the present effort to develop the HPLC–MS method to quantify the dalbavancin degradation products described in the "Materials and methods" section.

The dual aims of this study were to determine the structures of the major degradation products of dalbavancin under heat stress and to investigate the effect of divalent metal ions and 2HPβCD on the profiles of these degradants under such conditions. The decomposition of dalbavancin in various formulations was analyzed after incubation at 70 °C for 5 days and 3 days in acetate (pH 4.5) and phosphate (pH 7.0) buffer, respectively.

The analysis identified two known impurities, mannosyl aglycone (MAG) and DB-R2, and four previously unreported degradants. MAG, the major degradation product, was formed by hydrolysis of the glycosidic linkage to the side chain of residue 4 of the dalbavancin peptide (Stogniew et al. 2012). A similar degradation had been reported for other, related glycopeptides (Liu et al. 2011; Eugenia and Anna 2017).

In addition to the known degradation products, two pairs of diastereomers with identical molecular masses but different retention times were labeled as degradation products DB-DP1 and DB-DP2. Characterization by LC–MS-MS showed that DB-DP2 and its diastereomer DB-Iso-DP2 were formed by hydrolytic deamination of the methylamine group on residue 1 of the cyclopeptide, and that DB-DP1 and DB-Iso-DP1 were formed respectively from DB-DP2 and DB-Iso-DP2 by hydrolytic cleavage of the glycosidic linkage at residue 4 of the peptide.

Secondary and tertiary MS fragmentation studies strongly suggested that the stereoisomer pairs were epimers of the alpha carbon of residue 3, by analogy with the known structures of dalbavancin and the DB-R2 impurity. Residue 3, like residues 4, 5, and 7 of the dalbavancin peptide, is the noncanonical amino acid phenylglycine, which occurs in nearly all glycopeptide antibiotics (Al Toma et al. 2015). Because phenylglycine

(See figure on next page.)

Fig. 8 Molecular structures of **a** MAG, **b** DB-R2[a], **c** DB-DP2[b], **d** DB-Iso-DP2[c], **e** DB-DP1[d], and **f** DB-Iso-DP1[e], produced by the thermal degradation of dalbavancin in acetate and phosphate-buffered solutions. (**a**. DB-R2 impurity was formed in Phosp10Cyclod110 and Phosp10Mg50Cyclod110 degraded samples. **b**. DB-DP2 (3*S*,4*R*,5*R*,6*S*)-6-{[(1*S*,2*R*,34*S*,37*R*,40*R*,52*S*)-5,32-dichloro-52-{[3-(dimethylamino)propyl]carbamoyl}-2,22,26,31,44,49-hexahydroxy-21,35,38,54,56,59-hexaoxo-47-{[(2*R*,3*S*,4*S*,5*S*,6*R*)-3,4,5-trihydroxy-6-(hydroxymethyl)oxan-2-yl]oxy}-7,13,28-trioxa-20,36,39,53,55,58-hexaazaundecacyclo[38.14.2.2^{3,6}.2^{14,17}.2^{19,34}.1^{8,12}.1^{23,27}.1^{29,33}.1^{41,45}.0^{10,37}.0^{46,51}]hexahexaconta-3,5,8(64),9,11,14,16,23(61),24,26,29(60),30,32,41(57),42,44,46,48,50,62,65-henicosaen-64-yl]oxy}-3,4-dihydroxy-5-(10-methylundecanamido)oxane-2-carboxylic acid. **c**. DB-Iso-DP2 (3*S*,4*R*,5*R*,6*S*)-6-{[(1*S*,2*R*,34*R*,37*R*,40*R*,52*S*)-5,32-dichloro-52-{[3-(dimethylamino)propyl]carbamoyl}-2,22,24,26,31,44,49-heptahydroxy-21,35,38,54,56,59-hexaoxo-47-{[(2*R*,3*S*,4*S*,5*S*,6*R*)-3,4,5-trihydroxy-6-(hydroxymethyl)oxan-2-yl]oxy}-7,13,28-trioxa-20,36,39,53,55,58-hexaazaundecacyclo[38.14.2.2^{3,6}.2^{14,17}.2^{19,34}.1^{8,12}.1^{23,27}.1^{29,33}.1^{41,45}.0^{10,37}.0^{46,51}]hexahexaconta-3,5,8(64),9,11,14,16,23(61),24,26,29(60),30,32,41(57),42,44,46,48,50,62,65-henicosaen-64-yl]oxy}-3,4-dihydroxy-5-(10-methylundecanamido)oxane-2-carboxylic acid. **d**. DB-DP1 (1*S*,2*R*,34*S*,37*R*,40*R*,52*S*)-5,32-dichloro-*N*-[3-(dimethylamino)propyl]-2,22,26,31,44,49,64-heptahydroxy-21,35,38,54,56,59-hexaoxo-47-{[(2*R*,3*S*,4*S*,5*S*,6*R*)-3,4,5-trihydroxy-6-(hydroxymethyl)oxan-2-yl]oxy}-7,13,28-trioxa-20,36,39,53,55,58-hexaazaundecacyclo[38.14.2.2^{3,6}.2^{14,17}.2^{19,34}.1^{8,12}.1^{23,27}.1^{29,33}.1^{41,45}.0^{10,37}.0^{46,51}]hexahexaconta-3,5,8(64),9,11,14,16,23(61),24,26,29(60),30,32,41(57),42,44,46,48,50,62,65-henicosaene-52-carboxamide. **e**. DB-Iso-DP1 (1*S*,2*R*,34*R*,37*R*,40*R*,52*S*)-5,32-dichloro-*N*-[3-(dimethylamino)propyl]-2,22,26,31,44,49,64-heptahydroxy-21,35,38,54,56,59-hexaoxo-47-{[(2*R*,3*S*,4*S*,5*S*,6*R*)-3,4,5-trihydroxy-6-(hydroxymethyl)oxan-2-yl]oxy}-7,13,28-trioxa-20,36,39,53,55,58-hexaazaundecacyclo[38.14.2.2^{3,6}.2^{14,17}.2^{19,34}.1^{8,12}.1^{23,27}.1^{29,33}.1^{41,45}.0^{10,37}.0.^{46,51}]hexahexaconta-3,5,8(64),9,11,14,16,23(61),24,26,29(60),30,32,41(57),42,44,46,48,50,62,65-henicosaene-52-carboxamide)

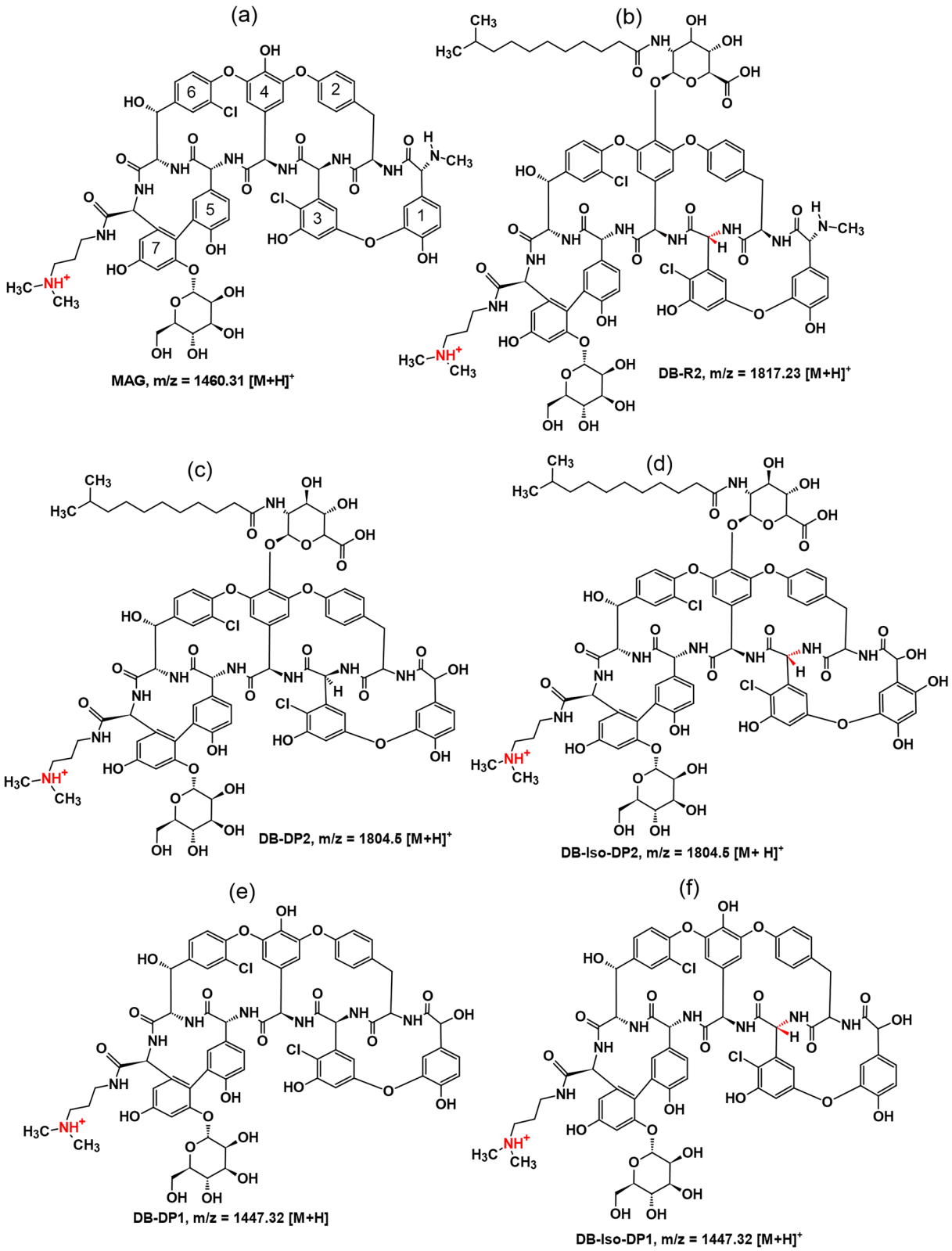

Fig. 8 (See legend on previous page.)

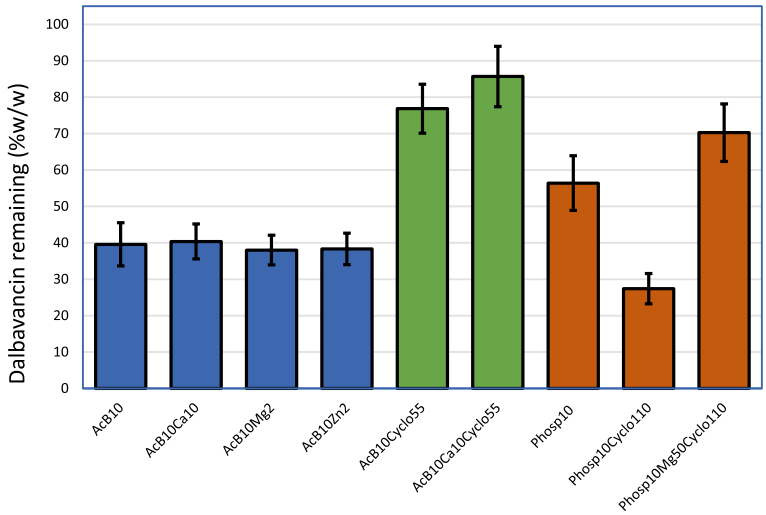

Fig. 9 Dalbavancin recovery by LC–MS after 5 days at 70 °C in 10 mM acetate buffer (pH 4.5) with no ions, 10 mM Ca^{2+}, 2 mM Mg^{2+}, and 2 mM Zn^{2+} (blue bars); with 55 mM 2HPβCD and 0 mM or 10 mM Ca^{2+}(green bars); and after 3 days at 70 °C in 10 mM phosphate buffer with 110 mM 2HPβCD and 0 mM or 50 mM Mg^{2+} (orange bars). The results are depicted as averages of three independent measurements ± SD

Table 4 The effect of divalent metal ions on the yields of degradation products of dalbavancin found after stressing at 70 °C for 5 days in 10 mM acetate buffer

Compound ID	Relative EIC peak intensity (%)[a]			Fraction of total HPLC-UV peak area (%)[b]			
	AcB10Ca10	AcB10Mg2	AcB10Zn2	AcB10	AcB10Ca10	AcB10Mg2	AcB10Zn2
MAG	105	99	101	51.2	53.6	50.5	49.0
DB-Iso-DP1	73	96	60	0.97	0.71	0.92	0.61
DB-DP1	96	97	74	0.77	0.62	0.76	0.62
DB-Iso-DP2	76	98	68	1.6	1.2	1.6	1.1
DB-DP2	85	99	69	1.1	0.90	1.1	0.76
Dalbavancin (B0)	91	97	106	39.5	38.7	39.9	42.1
Unknown degradants	None detected	None detected	None detected	4.9	4.3	5.1	2.5
Total degradants	N/A	N/A	N/A	60.6	61.3	60.0	58.1

[a] Levels of degradation products are expressed relative to their levels in acetate buffer without metal ions

[b] Levels of degradation products are expressed as the area under their HPLC peak as a percentage of the total peak area

is susceptible to racemization due to the acidity of the hydrogen on its alpha carbon (Nicolaou et al. 1999), this is a likely site for epimerization to occur.

Since no acetate adducts with dalbavancin were detected, it is likely that free acetate in the solution does not interact directly with dalbavancin. The combination of acetate buffer and divalent metal ions did not reduce the formation of MAG although it did reduce the relative amounts of DB-DP1, DB-DP2, and their diastereomers. Since these compounds were present in a very low amount (< 2%), this reduction did not significantly affect the overall amount of dalbavancin degradation. Wyttenbach et al. (Wyttenbach et al. 2008) found that under acidic conditions (pH 3.0), divalent metal ions bind to the carbonyl groups in the ring structure of oxytocin. The present finding that MAG formation was not inhibited by divalent metal ions suggests that the interaction of dalbavancin and divalent metal ions in acetate buffer may be much weaker or not sterically favored.

While Ca^{2+}, Mg^{2+}, and Zn^{2+} were ineffective in reducing MAG formation in acetate buffer, 2HPβCD in acetate buffer strongly decreased MAG formation. The same conclusion was drawn in our previous long-term study at lower temperatures, where the presence of 2HPβCD protected dalbavancin from degradation over 6 months at 40 °C. Granados et al. (Granados and Rossi 2001) studied the effect of 2HPβCD on the intramolecular catalysis of amide hydrolysis of phthalamic acid and found

Table 5 The effect of 2HPβCD with and without Ca^{2+} on the yields of degradation products of dalbavancin found after stressing at 70 °C for 5 days in 10 mM acetate buffer

Compound ID	Relative EIC peak intensity[a] (%)		Fraction of total HPLC-UV peak area[b] (%)		
	AcB10Cyclod55	AcB10 Ca10Cyclod55	AcB10	AcB10Cyclod55	AcB10Ca10Cyclod55
MAG	79	68	51.2	40.1	34.9
DB-Iso-DP1	143	176	0.97	1.4	1.74
DB-DP1	31	38	0.77	0.23	0.34
DB-Iso-DP2	129	198	1.6	2.1	3.3
DB-DP2	29	44	1.1	0.26	0.40
Dalbavancin (B0)	125	158	39.5	50.9	54.0
Unknown degradants	None detected	None detected	4.9	5.0	5.3
Total degradants	N/A	N/A	60.6	49.1	46.0

[a] Levels of degradation products are expressed relative to their levels in acetate buffer without metal ions

[b] Levels of degradation products are expressed as the area under their HPLC peak as a percentage of the total peak area

Table 6 The effect of 2HPβCD with and without Mg^{2+} on the yields of degradation products of dalbavancin found after stressing at 70 °C for 3 days in 10 mM phosphate buffer

Compound ID	Relative EIC peak intensity (%)		Fraction of total HPLC-UV peak area (%)		
	Phosp10Cyclod110	Phosp10Mg50Cyclod110	Phosp10	Phosp10Cyclod110	Phosp10Mg50Cyclod110
MAG	40	117	11.1	7.4	15.2
DB-Iso-DP1	135	142	1.9	2.4	2.4
DB-DP1	174	130	0.82	0.9	0.7
DB-R2	1267	240	0.74	6.6	1.7
DB-Iso-DP2	216	148	7.2	14.2	9.3
DB-DP2	268	146	1.8	3.3	2.0
Dalbavancin (B0)	70	97	64.1	45.9	60.2
Unknown degradants	None detected	None detected	7.0	16.9	5.6
Total degradants	N/A	N/A	30.6	51.7	36.2

that 2HPβCD strongly inhibited the hydrolysis by a factor of at least 10–30 by complexing phthalamic acid into the cyclodextrin cavity. By analogy, it seems likely that 2HPβCD in acetate buffer inhibited glycosidic hydrolysis of dalbavancin by forming a complex in the region where the degradation reaction occurs. An obvious candidate for the site of interaction with the hydrophobic center of the cyclodextrin is the aliphatic tail of the glycone moiety attached to residue 4.

The addition of Ca^{2+} significantly enhanced the stabilizing effect of 2HPβCD in acetate at 70 °C in the present study. This result differed from our previous study under accelerated conditions at 40 °C for 6 months, in which the addition of Ca^{2+} ion increased dalbavancin recovery by only ~ 3% relative to 2HPβCD in acetate alone. A possible explanation for the much greater effect of Ca^{2+} at the higher temperature is that Ca^{2+} may raise the activation energy for the glycosidic bond hydrolysis. A higher activation energy would give hydrolysis in the presence of Ca^{2+} ion a steeper temperature dependence than in its absence, so that hydrolysis in the presence of Ca^{2+} could become more competitive at higher temperatures. Since Ca^{2+} is known to bind strongly with carbohydrates functionalized with a carboxyl group (Bazin et al. 1995), an obvious possible interaction site for Ca^{2+} is the carboxyl on the carbohydrate moiety of the glycone tail, which is immediately adjacent to the anomeric carbon where glycosidic bond cleavage occurs.

The present results also showed that Ca^{2+} significantly enhanced the protective effect of 2HPβCD and further reduced the formation of MAG under heat stress. This could be due to a cooperative interaction of 2HPβCD and Ca^{2+} that strengthens the binding of the cyclodextrin to dalbavancin or to a direct effect of Ca^{2+} on the glycolytic cleavage via interaction with the carboxyl group of the glycone as discussed above.

Table 7 Comparison of dalbavancin degradation products in different formulations at 70 °C and 40 °C

	AcB10	AcB10Ca10	AcB10Mg2	AcB10Zn2	AcB10Cyclod55	AcB10Ca10Cyclod55	Phosp10	Phosp10Cyclod110	Phosp10Mg50Cyclod110
70 °C study									
MAG	51.2	53.6	50.5	49	40.1	34.9	11.1	7.4	15.2
DB-R2							0.74	6.6	1.7
DB-R6									
DB-Iso-DP1	0.97	0.71	0.92	0.61	1.4	1.7	1.9	2.4	2.4
DB-DP1	0.77	0.62	0.76	0.62	0.23	0.34	0.82	0.9	0.7
DB-Iso-DP2	1.6	1.2	1.6	1.1	2.1	3.3	7.2	14.2	9.3
DB-DP2	1.1	0.9	1.1	0.76	0.26	0.4	1.8	3.3	2
Unknown	4.9	4.3	5.1	2.5	5	5.3	7	16.9	5.6
Dalbavancin[a]	39.5	38.7	39.9	42.1	50.9	54	64.1	45.9	60.2
All degradants	60.5	61.3	60.0	54.6	49.1	46.0	30.6	51.7	36.9
40 °C study									
MAG	41.8	40.3	42	42.3	24	24.3		3.9	6.1
DB-R2	0.23			0.24				6.5	3.0
DB-R6	0.68				0.25	0.23		0.85	0.47
DB-Iso-DP1									
DB-DP1									
DB-Iso-DP2	0.61	0.77	0.62	0.59	0.96	0.85		4.1	3.2
DB-DP2									
Unknown								0.55	
Dalbavancin	48	51	49	49	71	71		50	66
All degradants	43.3	41.1	42.6	43.1	25.2	25.4		15.9	12.8

[a] Major B0 isoform only

Interestingly, 2HPβCD in acetate either with or without Ca^{2+} also reduced the formation of the DB-DP1 and DB-DP2 degradants, but not their stereoisomers. This suggests that epimerization of the residue 3 alpha carbon could lead to large-scale changes in the conformation of the peptide macrocycle such that the conformations of DB-Iso-DP1 and DB-Iso-DP2 are disfavored by steric interactions with the cyclodextrin.

In phosphate buffer, the much higher recovery of dalbavancin compared to that in acetate buffer either with or without divalent metal ions may seem surprising. However, it must be recalled that dalbavancin, although soluble in the method diluent used in the HPLC analysis, was virtually insoluble in phosphate buffer at pH 7.0. In its aggregated state, dalbavancin is most likely protected from chemical attack in solution, leading to a higher observed recovery of the drug. Similar to the situation in acetate buffer, the addition of 2HPβCD did reduce the formation of MAG, which suggests that it may also sterically hinder hydrolysis of the glycosidic bond in this case. The fact that 2HPβCD solubilized dalbavancin in phosphate buffer at pH 7.0 also suggests that it must interact with the aliphatic glycone tail. However, 2HPβCD greatly increased the formation of unidentified degradants and that of DB-R2 by more than tenfold, which resulted in a lower overall recovery of dalbavancin compared to phosphate buffer alone.

The effect of adding Mg^{2+} to 2HPβCD in phosphate contrasted starkly with the combined effect of Ca^{2+} and 2HPβCD in acetate: MAG formation was increased in this formulation relative to buffer alone. This suggests that the steric interaction of the cyclodextrin with dalbavancin is very different in the two cases and supports the idea that 2HPβCD may bind cooperatively to dalbavancin with Ca^{2+} but not with Mg^{2+}. However, the addition of Mg^{2+} did significantly reduce the formation of unknown degradants DB-R2 and DB-Iso-DP2 relative to 2HPβCD alone, resulting in an overall increase in dalbavancin stability, as shown in Fig. 9 and consistent with previous results.

Although no direct interaction between dalbavancin and phosphate was detected by MS, the DB-R2 epimerized product was only detectable in the phosphate buffer and dramatically increased with the addition of 2HPβCD. It may be that phosphate ion is a strong enough base to remove the hydrogen on the alpha carbon of residue 3, and steric interaction with 2HPβCD causes a conformational change that further exposes this carbon to attack.

Whereas the analysis of the product yields at 70 °C offers insights into how different excipients affect the degradation chemistry of dalbavancin, the comparison to the product yields at 40 °C establishes the relevance of those results to results obtained at standardized testing conditions. Every product observed at 40 °C except for DB-R6 could be characterized at a higher temperature. Three additional products appeared at 70 °C, presumably because the more rigorous conditions promoted further reactions. These reactions are simply extensions of the pathway that produces DB-R2 and DB-Iso-DP2 at 40 °C, which can be seen from the structures in Fig. 7 and the schematic diagram in Fig. 10. At 70 °C, DB-DP2 is formed via the epimerization, which may also occur undetectably at 40 °C. These reactions are followed by the loss of the MAG group on ring 3 to form the DB-DP1 stereoisomers.

The absence of DB-R6 in the 70 °C studies is not the exception it first appears to be. DB-R6 is formed from dalbavancin at 40 °C by the loss of the mannosyl group on ring 7. This group is eventually lost in the further reactions at 70 °C, but the loss of the groups at the N-terminus and ring 3 must be so much faster than the loss of the mannosyl group at 70 °C that DB-R6 is never observed. Because the reactions that form additional products at 70 °C are extensions of the 40 °C reaction pathways, these products are also relevant in that they should represent degradations that may be expected under the even more extreme temperatures that sometimes arise during the shipment of pharmaceuticals in climate regions III and IV.

Conclusions

Solution stability is a significant issue for dalbavancin (Stogniew et al. 2012) which is why it, like other glycopeptide drugs, is only distributed in lyophilized form. The general availability of this important antibiotic is therefore limited, highlighting the need to develop a formulation that would significantly extend its long-term stability in solution. This first HPLC–MS. characterization of dalbavancin stability in heat-stressed solution formulations has identified four previously unreported degradation products in addition to two degradants that had already been characterized. HPLC–MS profiling of these products with different buffers, divalent metal ions, and 2HPβCD has provided new information that will help to elucidate the chemical processes involved in the heat decomposition of dalbavancin in solution. The most significant observation from this work was that 2HPβCD greatly inhibited the hydrolysis reaction that forms the major degradation product, mannosyl aglycone (MAG), even under extreme heat stress. In fact, 2HPβCD appears to provide long-term thermal stability for dalbavancin

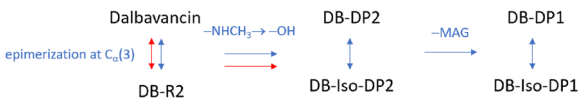

Fig. 10 Schematic comparison of the degradation pathways at 40 °C and 70 °C. Red arrows indicate the processes that are observed at 40 °C, and blue arrows indicate processes that are observed at 70 °C

in both acetate and phosphate buffers. Kinetic studies of degradation reactions in the presence of 2HPβCD are underway to determine the shelf life of this formulation at room and elevated temperatures more accurately. This dramatic improvement in stability opens the practical possibility of a much wider distribution of this important antibiotic to developing countries in tropical climates.

Another important finding was the identification of a common pathway in dalbavancin degradation, namely epimerization of the alpha carbon of residue 3, a phenylglycine. This modification appeared to induce a conformation change in the dalbavancin macrocycle that may eliminate its efficacy entirely. Finally, acetate-buffered dalbavancin solutions were more stable than phosphate-buffered solutions; only 2% or less of these epimerized products were observed in acetate-buffered solutions. Interestingly, some other known degradation products of dalbavancin were not observed in this heat degradation study, and further work is required to understand their formation. Such understanding will undoubtedly enable yet further improvements in dalbavancin stability in solution.

Supplementary Information

The online version contains supplementary material available at https://doi.org/10.1186/s41120-023-00076-7.

Additional file 1.

Acknowledgements
This research work was supported by Hikma Pharmaceuticals.

Authors' contributions
The authors confirm their contributions to the paper as follows: Research work was conducted in the lab, and the manuscript was prepared by SMJ. DEB and JM critically reviewed and revised the draft for intellectual content. All authors reviewed, edited, and approved the final version of the manuscript.

Funding
The authors have received no payment for the preparation of this manuscript.

Availability of data and materials
Not applicable.

Declarations

Competing interests
The authors declare that they have no competing interests.

Received: 5 October 2022 Accepted: 10 March 2023
Published online: 04 April 2023

References

Al Toma RS, Brieke C, Cryle MJ, Süssmuth RD (2015) Structural aspects of phenylglycines, their biosynthesis and occurrence in peptide natural products. Nat Prod Rep 32:1207-1235
Alebic-Kolbah T, Demers R, Cojocaru L (2011) Dalbavancin: quantification in human plasma and urine by a new improved high performance liquid chromatography–tandem mass spectrometry method. J Chromatogr B Analyt Technol Biomed Life Sci 879(25):2632-2641
Avataneo V, Antonucci M, De Vivo ED, Briozzo A, Cusato J, F. Bermond F et al (2021) Validation and clinical application of a new liquid chromatography coupled to mass spectrometry (HPLC-MS) method for dalbavancin quantification in human plasma. Separations 8:189
Bazin H, Bouchu A, Descotes G, Petit-Ramel M (1995) Comparison of calcium complexation of some carboxylic acids derived from D-glucose and D-fructose. Can J Chem 73:1338–1347
Belissa E, Nino C, Bernard M, Henriet T, Sadou-Yaye H, Surget E et al (2014) Liquid chromatography–tandem mass spectrometry for simultaneous determination of ticarcillin and vancomycin in presence of degradation products. Application to the chemical stability monitoring of ticarcillin-vancomycin solutions. J Chromatogr Sep Tech. 5:5
Blaskovich MAT, Hansford KA, Butler MS, Jia Z, Mark AE, Cooper MA (2018) Developments in glycopeptide antibiotics. ACS Infect Dis 4:715–735
Cao M, Feng Y, Zhang Y, Kang W, Lian K, Ai L (2018) Studies on the metabolism and degradation of vancomycin in simulated in vitro and aquatic environment by UHPLC-Triple-TOF-MS/MS. Nat Sci Rep. 8:15471
Cheng M, Ziora ZM, Hansford KA, Blaskovich MA, Butler MS, Cooper MA (2014) Anti-cooperative ligand binding and dimerisation in the glycopeptide antibiotic dalbavancin. Org Biomol Chem 12:2568–2575
DALVANCE, Dalbavancin injection, powder, lyophilized for solution [package insert]: Durata Therapeutics Inc; 2014 [Available from: https://dailymed.nlm.nih.gov/dailymed/drugInfo.cfm?setid=4b4674d8-4d1e-4728-8465-d42ada33fa5c]
Eugenia NO, Anna NT (2017) Synthesis, Properties, and mechanism of action of new generation of polycyclic glycopeptide antibiotics. Med Chem. 17:1–33
Giurazza R, Mazza MC, Andini R, Sansone P, Pace MC, Durante-Mangoni E (2021) Emerging treatment options for multi-drug-resistant bacterial infections. Life (basel) 11(6):519
Granados AM, de Rossi RH (2001) Effect of cyclodextrin on the intramolecular catalysis of amide hydrolysis. J Org Chem 66:1548–1552
Grimm W (1998) Extension of the international conference on harmonization tripartite guideline for stability testing of new drug substances and products to countries of climatic zones III and IV. Drug Dev Ind Pharm. 24:313–25
Huber R, Marcourt L, Quiros-Guerrero L-M, Chiriac CU (2022) Validation and application of an HPLC-UV method for routine therapeutic drug monitoring of dalbavancin. Antibiotics 11(5):541
Leuthner KD, Buechler KA, Kogan D, Saguros A, Lee HS (2016) Clinical efficacy of dalbavancin for the treatment of acute bacterial skin and skin structure infections (ABSSSI). Therapeut Clin Risk Manage 12:931–40
Liu J, Lee J, inventors; Theravance Inc:, assignee (2011) Hydrochloride salts of a glycopeptide phosphonate derivative. USA patent US8003755
Malabarba A, Ciabatti R (2001) Glycopeptide derivatives. Curr Med Chem 8:1759–1773
Nicolaou KC, Boddy CNC, Bräse S, Winssinger N (1999) Chemistry, biology, and medicine of the glycopeptide antibiotics. Angew Chem Int Ed 38:2096–2152
Poole RA, Kasper PT, Jiskoot W (2011) Formation of amide- and imide-linked degradation products between the peptide drug oxytocin and citrate in citrate-buffered formulations. J Pharm Sci. 100:3018–22
Scheinfeld N (2006) Dalbavancin: a review for dermatologists. Dermatol Online J 12(4):6
Stogniew M, Colombo L, R. C, inventors; Vicuron Pharmaceuticals LLC, assignee. (2012) Dalbavancin compositions for treatment of bacterial infections patent US8143212B2
Wyttenbach T, Liu D, Bowers MT (2008) Interactions of the hormone oxytocin with divalent metal ions. J Am Chem Soc. 130:5993–6000
Zhu D, Ping L, Hong Y, Shen J, Weng Q, He Q (2020) Simultaneous quantification and pharmacokinetic study of five homologs of dalbavancin in rat. Molecules 25:4100
Ziora ZM, Hansford K, Blaskovich M, Butler MS (2014) Anti-cooperative ligand binding and dimerization in the glycopeptide antibiotic dalbavancin. Org Biomolec Chem. 12(16):2568–75

Publisher's Note